# Investigating the effects of kinetic hydrate inhibitors and antifreeze glycoproteins in inhibiting the growth of THF hydrates

Presented to the S. Daniel Abraham Honors Program in Partial Fulfillment of the Requirements for Completion of the Program

Atara Neugroschl

Stern College for Women, Yeshiva University

May 20, 2022

Mentor: Dr. Ran Drori, Department of Chemistry and Biochemistry

# Table of Contents

1. Introduction ..... 2

1.1: What are clathrate hydrates? ..... 2

1.2: Clathrate hydrate inhibitors ..... 3

1.3: Tetrahydrofuran (THF) as a model crystal ..... 6

1.4: Research hypotheses and aims ..... 9

2. Mechanism of Hydrate Inhibitors ..... 9

2.1: Antifreeze protein inhibition mechanism and the Gibbs-Thomson Effect ..... 9

2.2: Hydrate surface interactions and properties of polyvinylpyrrolidone (PVP) and PVCap . 12

2.3: Zirconium acetate hydroxide properties and inhibition ..... 14

3. Materials and Methods ..... 15

3.1: Experimental setup ..... 15

3.2: Experimental procedure ..... 16

4. Results ..... 18

4.1: Thermal hysteresis activity of PVP inhibitors on THF hydrates ..... 18

4.2: Thermal hysteresis activity of zirconium acetate hydroxide on THF hydrates ..... 19

4.3: Thermal hysteresis activity of antifreeze glycoproteins on THF hydrates ..... 21

4.4: TH activity of all inhibitors compared ..... 23

5. Discussion ..... 24

5.1: Discussion of inhibitor results ..... 24

5.2: Challenges with studying THF hydrates ..... 25

References ..... 27

## 1. Introduction

### 1.1: What are clathrate hydrates?

Clathrate (or gas) hydrates comprise organic gaseous molecules trapped in a cage of water molecules (Figure 1). These water molecules hydrogen bond to one another, forming a crystalline structure. Most known gas hydrates are methane hydrates, which form in environments with low temperatures and high pressure[1]. In fact, these hydrates are incredibly common with an estimated amount of over $10^{19}$ g of methane carbon trapped in methane hydrates[2].

Figure 1: Diagram of a methane hydrate

Due to these specific conditions, methane hydrates often form in deep waters and permafrost. These reservoirs of stable methane hydrates are lauded as an untapped potential for fuel and energy[1]. However, in addition to stable hydrates that form in the natural environment, methane hydrates form inside natural gas and oil pipes. Because of the high-pressure flow of gas through these cold pipes, and the presence of water, the hydrates are favored to form. These methane hydrates present major ecological and safety threats. Unlike other hydrocarbon hydrates, methane hydrates are denser and do not flow through the petroleum pipes[3]. Because the hydrates cannot move

Figure 2: Image of a methane hydrate buildup in an oil pipe

through the pipes, they instead cause the pipes to clog up, leading to explosions and oil spills (Figure 2)[4] .

This backup of methane hydrates serves as a major safety, ecological, and economic risk. Methane is a known greenhouse, contributing to climate change and global warming. When oil and natural gas pipes explode due to methane hydrate buildup, this causes the release of methane from the pipes. This phenomenon of hydrate buildup is responsible for many natural disasters, including the 1988 explosion of the Piper Alpha oil platform where 167 people died[5]. Most famously, methane hydrates were to blame in the 2010 explosion of the Deepwater Horizon, an oil drilling rig in the Gulf of Mexico. This oil spill, regarded as the largest oil spill in the history of marine oil drilling, took nearly three months to contain, due to the extreme methane hydrate buildup[6].

In addition to the environmental cost, the control of methane hydrates and the cleanup of methane hydrate associated explosion have had a major financial detriment. As of 2015, it was estimated that companies spent around $1 billion annually on controlling hydrate growth in pipes[5]. Additionally, cleanup from hydrate related explosions have major costs associated. For example, after The Deepwater Horizon explosion there was a record-breaking settlement paid to BP Exploration and Production which included $8.8 billion in damages of natural resources and $5.5 billion as a penalty for the Clean Water Act[6]. Between the safety, ecological, and economical effects of methane hydrate buildup, these hydrates present a major threat.

## 1.2: Clathrate hydrate inhibitors

To avoid these damaging effects, inhibitors are used in oil and gas pipes to prevent hydrate formation and accumulation. Currently, thermodynamic hydrate inhibitors (THIs) are being used,

which prevent the formation of hydrates by changing the chemical potential of water. These THIs, such as glycols and alcohols, can form hydrogen-bonds. Therefore, they compete with the methane for the water and prevent the water molecules from forming a cage around the methane molecules and creating a hydrate[3]. By doing so, they lower the temperature required to form a crystal, also known as the crystallization point[5].

However, this method of inhibition is costly and requires large storage facilities. Methanol, one of the most commonly used THIs for hydrate inhibition, is estimated to cost $220 million annually. Additionally, these inhibitors are only effective at large concentrations. Not only does this make the addition of THIs inconvenient and bulky, but storage of large quantities of methanol is expensive[3]. In addition to the size and price of THIs, these inhibitors pose their own threat to people and the environment. Most THIs are dangerous toxins for both living organisms and the environment. Therefore, there are risks to the workers that handle the materials, and for the environment if the pipes burst and the inhibitors are freed. Additionally, ethylene glycol, a common THI used, has been proven to cause harm to aquatic organisms.

Because of the risks of THIs, kinetic hydrate inhibitors (KHIs) have been developed. These inhibitors are a type of LDHI, or low-dose hydrate inhibitor. Instead of having competing hydrogen bonding, these inhibitors either lower the crystallization temperature, thereby delaying nucleation of the crystal, or control the growth of the crystal after nucleation. Unlike THIs, KHIs are inexpensive, safe, and more efficient. KHIs can be effective at low concentration, as small as 0.5% by weight. This is a significantly higher efficacy than THIs. This also contributes to their being more inexpensive because a smaller quantity is needed to be effective[5]. Some known KHIs include polyvinylpyrrolidone (PVP) and PVCap[7]. There have already been preliminary data of PVP as an inhibitor of clathrate hydrates[8].

In addition to THIs and KHIs, antifreeze proteins (AFPs) have been found to inhibit the growth of hydrates. AFPs are naturally occurring proteins, found first in *Antarctic Notothenioid* fish nearly 60 years ago. These proteins allow the fish to live at sub-zero temperatures and prevent freezing injuries and damage to the organisms. Since their original discovery, AFPs have been found in many organisms including insects, bacteria, fungi, and plants. Additionally, it is evident that these proteins serve in different functions in the various organisms, aside from simply preventing freezing damage. For example, some organisms secrete antifreeze proteins to prevent ice growth in the surroundings and allow for space for respiration, division, and nutrient uptake[9].

These AFPs also have a variety of shapes and molecular makeups, including a class of at least eight related proteins called antifreeze glycoproteins (AFGPs). These proteins, which were found in the original *Antarctic Notothenioid* fish and Artic cod, have a varying number of repeating units of Ala-Ala-Thr and a disaccharide, β-d-galactosyl-(1→3)-α-N-acetyl-d-galactosamine (Figure 3). Because of the unique presence of a carbohydrate in these proteins, referred to as AFGP1-8, they are given their own subcategory[10].

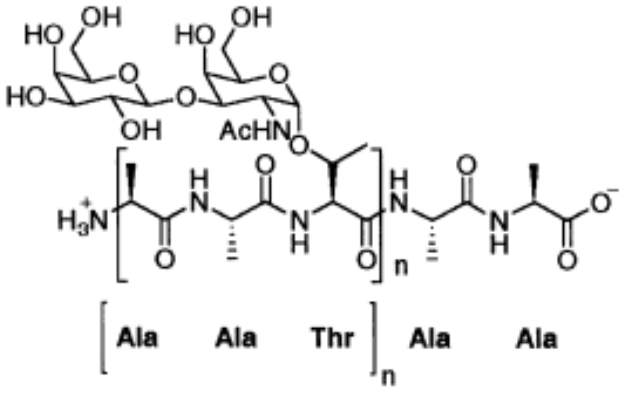

Figure 3: Structure of an AFGP molecule adapted from reference 10

While AFPs have been well categorized as ice inhibitors, there is evidence that they work as clathrate hydrate inhibitors as well. This presents an exciting possibility of a "green" inhibitor, meaning a clean method of hydrate inhibition. Unlike other inhibitors, AFPs are not known to be toxic to any organisms and are safe for humans handling the inhibitors. Additionally, because they

are proteins, if they were to be accidentally released, they are biodegradable and could be quickly hydrolyzed[5]. However, AFPs are costly, difficult to produce in large quantities, and have a shorter lifetime compared to other synthetic options[11].

1.3: Tetrahydrofuran (THF) as a model crystal

In this research project, instead of experimenting directly on methane hydrates, I used tetrahydrofuran (THF) hydrates as a model (Figure 4). As mentioned earlier, methane hydrates form under conditions of low temperatures and high pressure. These extreme conditions are expensive to achieve in a safe and stable form in the laboratory.

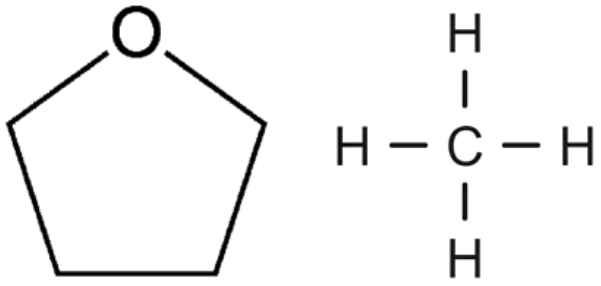

Figure 4: Structure of THF (left) and methane (right)

THF hydrates, on the other hand, form under standard conditions. These hydrates are formed using liquid THF, instead of gas molecules. The hydrates form at atmospheric pressure and at only a few degrees above 0 °C. Additionally, unlike methane hydrates that form only at the water-gas interface, THF hydrates form throughout the entire solution, because THF is miscible in water.

Methane and THF hydrates also differ in their structure shape. Hydrates have three main structure shapes: structure I (SI), structure II (SII), and structure H. The basic unit of each structure is a pentagonal dodecahedra, a 12-faced structure, with each face made up of 5 pentagonally bound water molecules[3]. SI is a body-centered cubit structure that tends to form around smaller molecules, between 0.4-0.55 nm, such as carbon dioxide and hydrogen sulfide. Therefore, these

types of hydrates are mostly found in the deep sea. SII is a diamond lattice inside a cubic frame, which forms with larger molecules, between 0.6-0.7nm, or those larger than ethane and smaller than pentane. These hydrates occur mainly in man-made environments or with thermogenic gases. Structure H hydrates have a mixture of small and large molecules (Figure 5).

Due to their size, methane hydrates form SI structures, while THF hydrates form SII structures. This divide is simply based on the molecule size and changing the ratios of molecule to water quantity has no effect on the hydrate structure. Additionally, occasionally a molecule is too large to fit inside all the water cages in a crystal structure. Therefore, instead of filling all the cages, they are only found in the larger ones, and the smaller ones are kept empty[1,3]. THF, because of its larger size, only fills the larger water cages while methane is found in both the large and small cages (Figure 6).

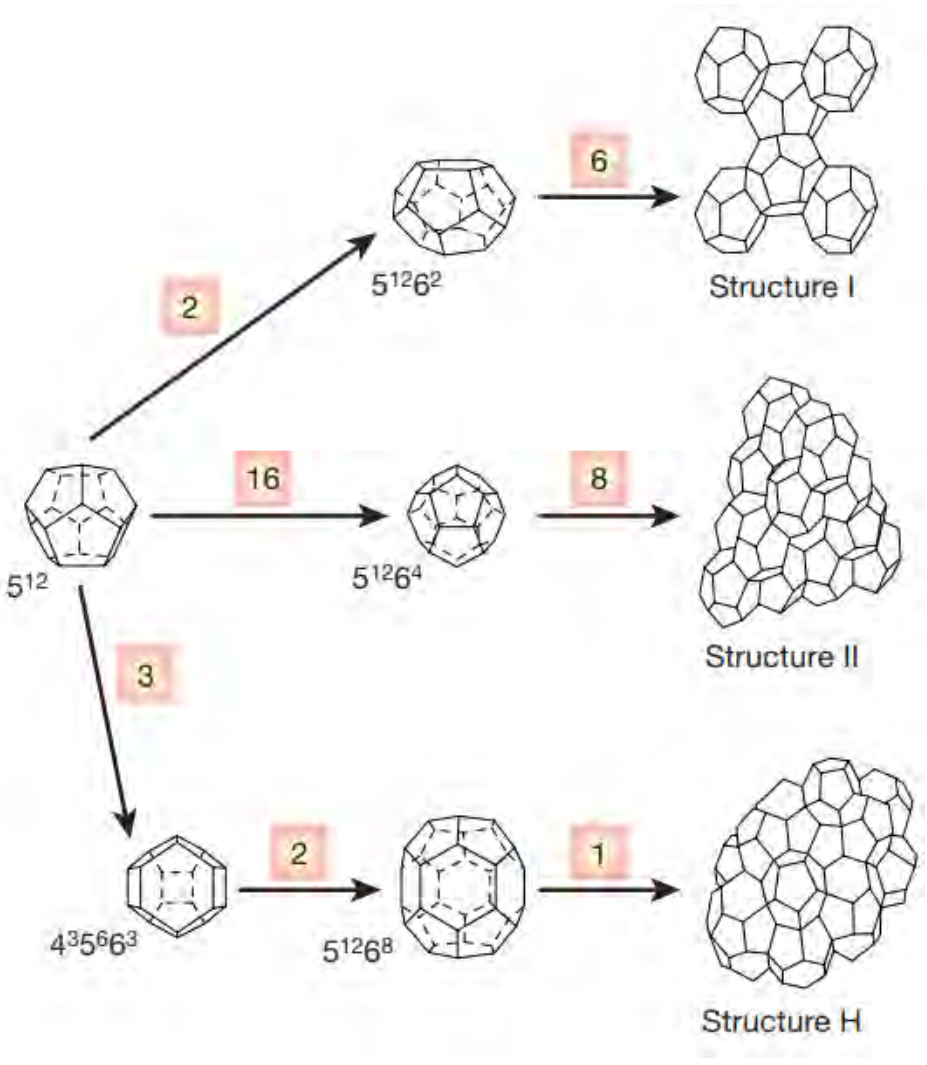


Figure 5: Schematic of crystal structures I, II, and H adapted from reference 3

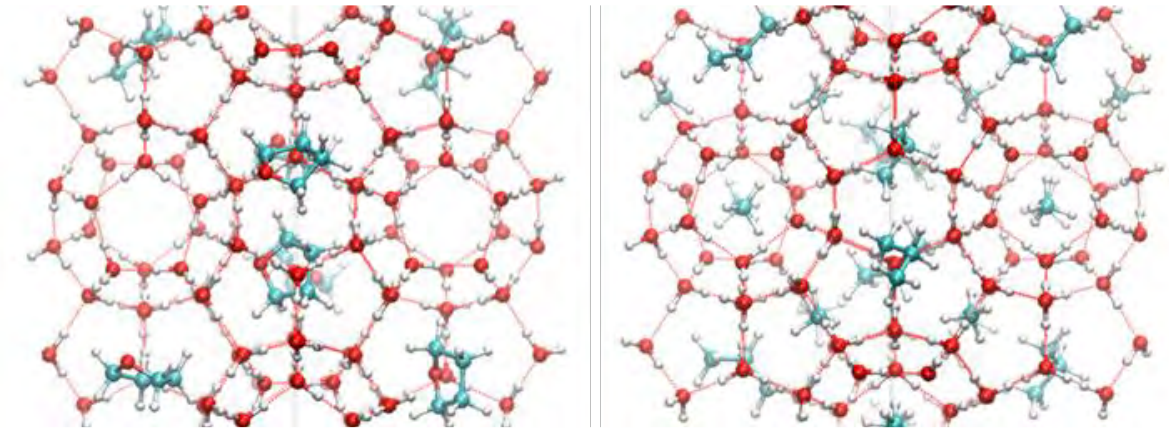

Figure 6: Schematic of THF hydrates (left) and methane hydrates (right) adapted from reference 12

In addition to hydrate structure, methane and THF hydrates differ in their polarity. Methane is a nonpolar hydrocarbon. This structure makes it immiscible in water and incapable of hydrogen bonding. In contrast, THF has an oxygen atom that gives the compound polarity. This allows THF to hydrogen bond and be miscible in water.

Despite these differences, THF hydrates have been used to study hydrocarbon hydrates due to their shared properties. Specifically, a study was done in 2019 by Vlasic et. al. exploring the use of THF as a substitute for methane. This study compared both compounds by looking at the atomic structures, vibrational properties, elastic properties, and crystal shapes. They measured these values of THF hydrates using density functional theory. These values were then compared to literature values for hydrocarbon clathrate hydrates. They concluded that the mechanical properties of THF hydrates were within the range of the values found for hydrocarbon hydrates. Specifically, they were nearly identical to the values obtained from methane and ethane hydrates. They also found that THF hydrates and hydrocarbon hydrates have the same structure-property relationships. Namely, the compressibility of both hydrates is dictated by the hydrogen bond density. Additionally, the guest molecules molecular weight is a function of the compressional wave velocity in both hydrates, and the hydrogen bond properties can be used to find the Young's

modulus. The study also failed to find evidence that the THF molecules were hydrogen bonding with water molecules, which was a concerning difference between THF and methane hydrates.

Therefore, the study concluded that on the basis of mechanical and structural properties, THF hydrates work as a viable substitute for methane hydrates. However, it is still unknown whether the difference in thermal properties or formation mechanism could cause major differences in the two hydrates and faults in using THF as a model[12].

### 1.4: Research hypotheses and aims

The effects of AFPs on ice have been studied more extensively, however, how KHIs inhibit the growth of hydrates is poorly understood. Therefore, based on my understanding of AFPs' mechanisms of inhibiting ice, my hypothesis was that KHI and AFPs with larger molecular weights will have higher TH activities. Using this hypothesis, I designed experiments to **examine the structure-activity relationship of these compounds**. I tested PVP at molecular weights of 10, 29, and 360 kDa. Additionally, I studied ZRAH and both large and small AFGPs, specifically AFGP8 and AFGP1-5. For each of these compounds, I measured the TH activity and various THF crystals and analyzed the structure-activity relationship. I hypothesized that these compounds would all be functional as inhibitors of THF hydrate, with the heavier molecules having the highest efficacy.

## 2. Mechanism of Hydrate Inhibitors

### 2.1: Antifreeze protein inhibition mechanism and the Gibbs-Thomson Effect

To understand how to inhibit the growth of clathrate hydrates, it is important to first understand how antifreeze molecules work. Specifically, AFPs which are naturally found proteins, are well characterized in their inhibition of ice. While it cannot be assumed that AFPs function

identically with clathrate hydrates as they do with ice molecule, understanding how AFPs work with ice gives a framework to begin studying inhibition of clathrate hydrates.

The mechanism by which AFPs inhibit ice growth, can be understood via the Gibbs–Thomson equation. According to the laws of Gibbs energy, the melting points of ice and water are equal. Therefore, in line with the second law of thermal dynamics, the following equations are true:

$G_{ice} = H_{ice} - TS_{ice}$ and $G_{water} = H_{water} - TS_{water}$

Because G = 0 at equilibrium, this concludes that:

$T_m$ (melting temperature) = $\Delta H / \Delta S$

According to this equation, it is evident that the melting point of ice is directly dependent on the entropy. Meaning an increase in entropy would cause a lowering of the melting point. This concept is evident in the freezing point depression effects of solutes in general. When dissolved in water, solutes cause a freezing point depression, and since this property is colligative, it is not dependent on the identity of the solute and any specific bonds or reactions that solute can form. Rather, it is simply a function of concentration. In fact, each osmole of solute, for the first several osmoles of a solute, depresses the melting point by about 1.86°C.

However, AFPs inhibit ice growth differently. Their antifreeze effects are not based on colligative properties. Rather, they bind to the surface of the ice. Therefore, the specific identity of the protein is key to its antifreeze capabilities. For example, *Tenebrio molitor* antifreeze proteins (*Tm*AFPs) are successful in depressing the freezing point of water by 2°C at only 0.00001 osmole.

When compared to salt, this is 100,000 times more effective by molarity, and 300 times more effective by weight. This stark increase in efficacy indicates that *Tm*AFPs are not depressing the freezing point based on colligative properties alone. Rather, through some other means, specific to the compound, they are able to affect the growth of ice.

One way AFPs affect the freezing point of ice is through the energy generated by surface tension on the ice-water interface. By analyzing the growth of ice crystals, the local curvature can be calculated. This number is the ratio between the addition to the surface area and the addition to the volume. The Gibbs-Thomson equation relates this curvature of the surface of the crystal to the temperature of the crystal during phase transition. The following is the Gibbs- Thomson equation:

$$T_m(r) = T_m(\infty) - 50\ \text{nm} \cdot {}^{\circ}\text{C}/r$$

In this equation, generated by Liu et. al. in 2003, r is the radius of curvature, $T_m(r)$ is the melting point of a curved surface with a radius of r, and $T_m(\infty)$ is the melting point of a flat surface. This equation explains why recrystallization occurs and why ice crystals remain stable when in a super cooled state. At a given temperature, crystals bigger than a given size grow, while those below a given size, shrink.

To explain further, in a growing crystal, water molecules can add on all sides to expand the crystal. Here the crystal has a flat surface and an infinite radius of curvature. However, when AFPs are added to the solution, they bind to the growing surface of the ice crystal. When AFPs are bound, they limit where the water molecules can bind. Therefore, water molecules that would bind to expand the crystal can only add between the proteins. Thus, instead of the case of a non-inhibited

protein, ice crystal growth continues until it reaches a critical radius and growth is no longer favored. Therefore, growth stops and only continues at a lower temperature (Figure 7).

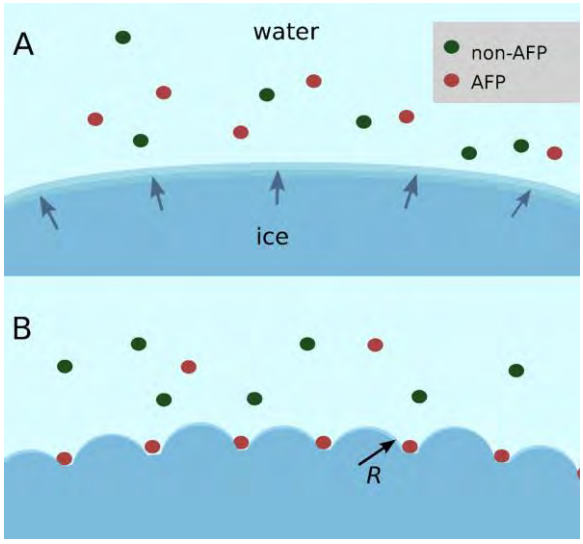


Figure 7: Schematic indicating how AFPs bind to the surface of ice adapted from Kuiper *et. al.* (2015)

Due to this property, inhibition via AFPs not only depresses the freezing point, but causes a gap between the melting temperature and freezing temperature of a crystal. This gap is known as the thermal hysteresis (TH). A hydrate crystal will melt at temperatures higher than its melting temperature and grow at temperatures lower than its freezing temperature. These two temperatures are essentially the same without inhibitors. However, in the presence of AFPs, the freezing point and melting point are separated, causing a TH[13].

2.2: Hydrate surface interactions and properties of polyvinylpyrrolidone (PVP) and PVCap

PVP and PVCap are synthetic polymers that have been identifies as LDHIs (Figure 8). Therefore, they have been studied as possible solutions to the accumulation of methane hydrates in oil pipes. These inhibitors cause the hydrates to form as platelike crystals.

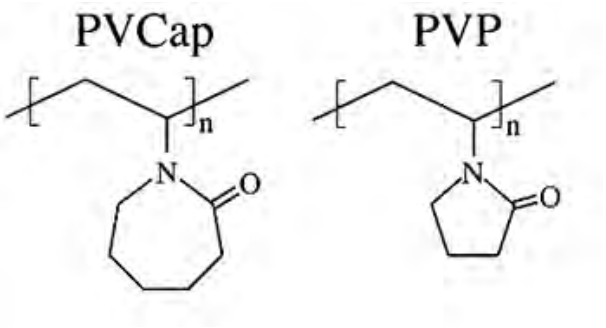


Figure 8: Structure of PVCap (left) and PVP (right)

PVP and PVCap inhibit hydrate growth through multiple methods. The first step of hydrate inhibition is preventing initial crystal nucleation. Crystal nucleation is an activated event and is

essentially an irreversible process. Once the hydrate gathers sufficient energy for nucleation, forming a small nucleus with a size in the order of tens of angstroms, crystal growth ensues. Therefore, the first way PVP and PVCap inhibit crystal growth is by disrupting the local organization of water and guest molecules so they need higher energy levels to overcome the inhibitors and nucleate.

After a crystal succeeds in nucleating, PVP and PVCap inhibit hydrates by binding to the hydrate's surface. The attached polymers slow crystal growth along the hydrate plane where they are bound. Additionally, the stronger the protein is bound to the hydrate surface, the more inhibited the crystal and the slower it grows. Specifically, inhibitors PVP, PVCap, and N-methyl,Nvinylacetamide (VIMA) were compared to a noninhibitor, PEO, in a study done by Anderson et. al. According to the study, the strength of binding is directly related to the inhibitors' binding free energy and the charge distribution.

When comparing the four compounds studied, they were most effective in the order of VIMA, PVCap, PVP, and then PEO. This directly corresponds to their binding energies, where the stronger inhibitors had more negative values. Specifically, their binding energies were -45.8, -37.5, -20.6, -0.2 kcal/mol respectively. They also had mostly increasingly favorable bonding free energies, with values of -15.1, -9.4, 0.5, 0.4 respectively. This indicates a neutral equilibrium constant for PEO and PVP, and a large equilibrium constant for PVCap and VIMA which would favor binding to the hydrate's surface.

The inhibitors' bond distributions also contribute to their functional abilities. PVP and PVCap have similar structure, and therefore have similar bond distributions. Both structures allow the inhibitors to form hydrogen bonds with the water molecules. However, PVCap has a larger ring than PVP. This causes the bond between the carbonyl carbon and its neighboring carbon on

the ring to be more rigid. This rigidity, in turn, allows PVCap to form stronger bonds than PVP[7]. Additionally, the larger size of PVCap allows the molecule to bind to more surface area than PVP[8]. These stronger bonds and the larger surface area covered, due to the structure of PVCap, result in PVCap being a more effective inhibitor than PVP.

Computer modeling has also been done to understand how PVP and PVCap bind to hydrates to inhibit growth. PVP was shown to bind irreversibly to the central parts of the hydrate cage, reducing the likelihood of gas getting trapped in the cage. PVCap, on the other hand, tends to form strong bonds along the surface of the hydrate where there are empty cages. While PVCap was seen to have stronger binding, the experiments were done on SII crystals, and it is unclear if the same would be true for SI crystals, such as methane hydrates[5].

In addition to PVCap being a stronger inhibitor compared to PVP, PVCap has been shown to be preferentially adsorbed onto hydrate surfaces. When studying cyclopentane hydrates in the presence of both PVP and PVCap, PVCap had a higher adsorption density, indicating a preference for PVCap surface binding over PVP[8]. Overall, PVP and PVCap were both shown to be effective LDHIs, with PVCap being a stronger inhibitor.

## 2.3: Zirconium acetate hydroxide properties and inhibition

Zirconium(IV) acetate hydroxide (ZRAH) is a synthetic material shown to share some properties of AFPs (Figure 9). Specifically, ZRAH prevents ice recrystallization and inhibits ice growth. When studied in the presence of ice, ZRAH presented some

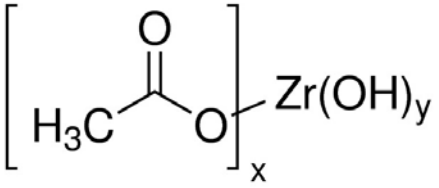


Figure 9: Structure of ZRAH

TH activity, indicating its potential for controlling ice growth[11]. However, studies of ZRAH as an inhibitor are new and no work has been done looking at ZRAH in the presence of hydrates.

## 3. Materials and Methods

### 3.1: Experimental setup

Other studies testing KHIs are limited to qualitative analysis that observes inhibitory effects on a macroscopic level. The apparatus used in these experiments is known as the copper cold-finger. A strip of copper is placed in a beaker containing the THF solution and the KHI of choice. Then the sample temperature is lowered in an insulated container. Because copper is an effective thermal conductor, it can maintain colder temperatures than the solution. Therefore, the surface of the copper finger serves as a platform for nucleation of ice crystals. These crystals can then be removed from the copper finger and studied. However, because of the macroscopic nature of these experiments, this method does not allow for an in-depth study of polymer size (molecular weight) on inhibition activity or for the comparison across different inhibitors[9].

I instead used a temperature-controlled cold stage, designed by my mentor, to study hydrates on a quantitative level. The cold stage itself is a copper plate situated inside a closed aluminum box, with a hole at the bottom to allow for light from the microscope to pass through. The cold plate rests on a Peltier thermoelectric cooler, which is governed by a temperature controller. A thermistor is inserted to a hole in the plate to measure the temperature and provide feedback to the temperature controller. The plate is fixed to a heat sink, that is attached to a water pump via Tygon tubes with an inner diameter of 4 mm. The water pump brings cold water through the box, and pumps warm water out, allowing for the removal of heat from the system. Nitrogen

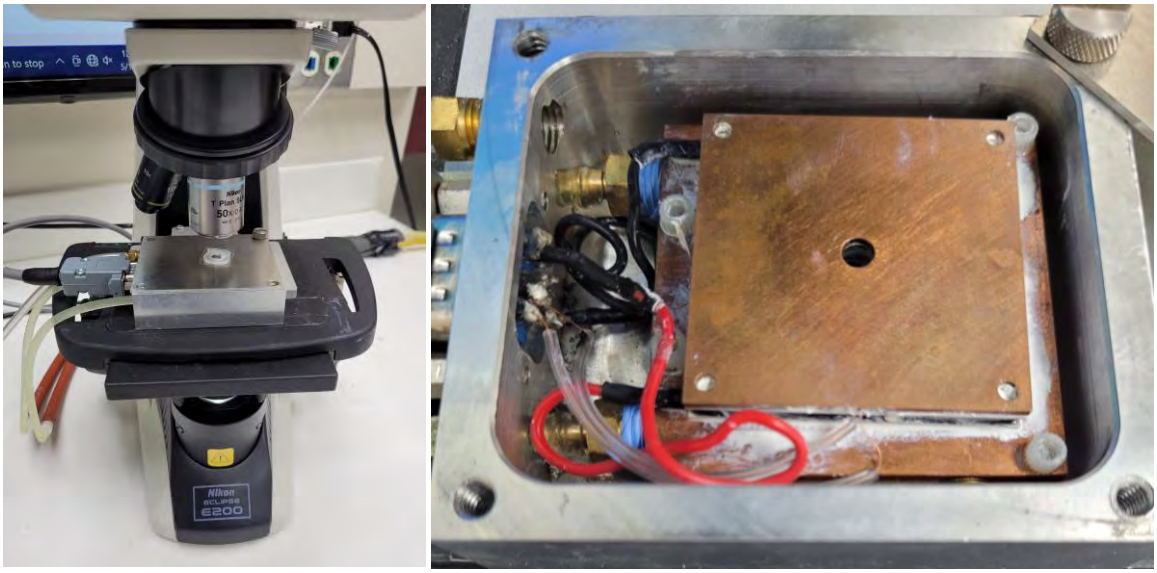


Figure 10: Image of the cooling stage including A) The cooling box connected to the microscope. B) The cooling box without the cover

gas is also connected via Tygon tubes to ensures the air inside the box is dry and condensation does not form.

A CMOS camera is mounted on the microscope, allowing for visualization of the sample inside the stage (Figure 10)[14]. Overall, this temperature-controlled cold stage allows me to isolate single microscopic hydrate crystals and observe their melting and freezing.

## 3.2: Experimental procedure

With the setup described above, I measured the TH activity of hydrates, which is the quantitative measurement of crystal growth inhibition. First, I inserted a small sample of the THF-inhibitor solution into the apparatus. To do this, I used a butane torch to melt a capillary tube until I produced a tapered end. Inserting the altered capillary tube at the end of a syringe, I then cut the tip of the closed tube until a small opening appeared. This opening was cut small enough to produce bubbles with less than a millimeter in diameter.

After preparing the capillary tube, I added a drop of immersion oil to the surface of a 1-inch diameter sapphire plate. Next, using the syringe and capillary tube, I aspirated a drop of the THF-inhibitor solution into the oil droplet. After adding the solution, I put a cover slip over the oil drop, trapping the sample in place. I then inserted the entire stack, including the sapphire plate, sample, and cover slip, on the temperature control stage in the microscope.

Once the solution was in place, I was able to use the temperature controller to freeze the entire sample. This usually occurred around -30 to -40°C. After the sample froze, I heated up the cold box, allowing the ice to melt off and leaving behind the frozen THF hydrates. By adjusting the temperature, I melted and grew the crystals until I isolated a single crystal.

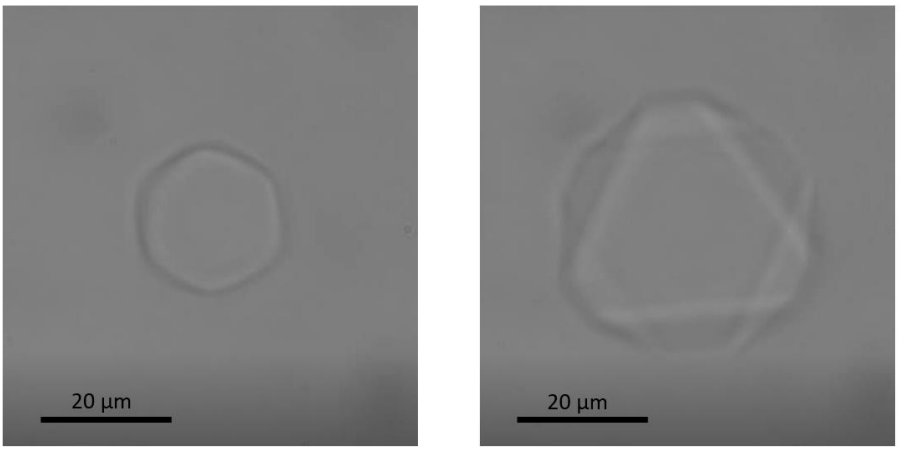


Figure 11: Pictures of crystal growth. On the left is a crystal at its melting point on the right is the same crystal at its bursting point

Once an individual THF crystal was identified, I measured the melting temperature of the crystal. This point was determined as the highest temperature that the crystal stops growing. The temperature resolution and stability of the cold stage is 1 mK, and therefore can precisely dictate the correct temperature. After recording the melting point, I set the program to lower the temperature by -0.05°C every 4 seconds. While the crystals slowly cooled, I observed both the shape and growth rate of the crystal. As noted earlier, THF hydrates tend to grow in distinct geometric formation when in the presence of hydrate

inhibitors. Next, I marked down the freezing point of the crystal. This was noted by the rapid burst of crystal growth, and therefore is sometimes referred to as the bursting point (Figure 11). By subtracting the temperature of the freezing point from the melting temperature, I determined the TH activity, which is a quantitative measurement of the efficacy of the inhibitor.

For each inhibitor concentration, I obtained at least five measurements, which were then averaged. These data points of average TH and concentration where then plotted in a graph indicating the trend in TH and inhibitor concentration. After obtaining a graph for a specific inhibitor, I varied the inhibitor's polymer size, and then compared the inhibition activity of the same compound at different molecular weights. Lastly, having tested different molecules, I also compared inhibition activity between different polymers and proteins. This allowed me to determine which inhibitor has the largest TH and is therefore the most effective inhibitor.

## 4. Results

### 4.1: TH activity of PVP inhibitors on THF hydrates

PVP10, PVP29, or PVP360 were added to a solution of water and THF. The three polymers were all tested at concentrations of 0.1, 0.5, 1, 2.5, 4, and 6 mg/mL. At each concentration, a minimum of five crystals were isolated and their TH was measured. I hypothesized that as the concentration increased, so would the inhibition activity. Additionally, I expected that the TH would increase as the molecular weight increases.

As seen in Figure 12, both hypotheses were confirmed. This graph shows the TH values corresponding to the square root of the molarity of the solution. I also compared the values I calculated with the values obtained from PVP40, that was tested earlier in the Drori lab[15]. In this instance, the square root was used in order to generate a linear graph. This way the data can be

more easily read and the different length PVP polymers can be compared. Using these linear lines, it is evident that with increased molarity, each polymer becomes more effective at inhibiting crystal growth. This is seen by the increasing TH. Additionally, with increasing polymer length, the PVP molecules became more effective and exhibit higher TH values.

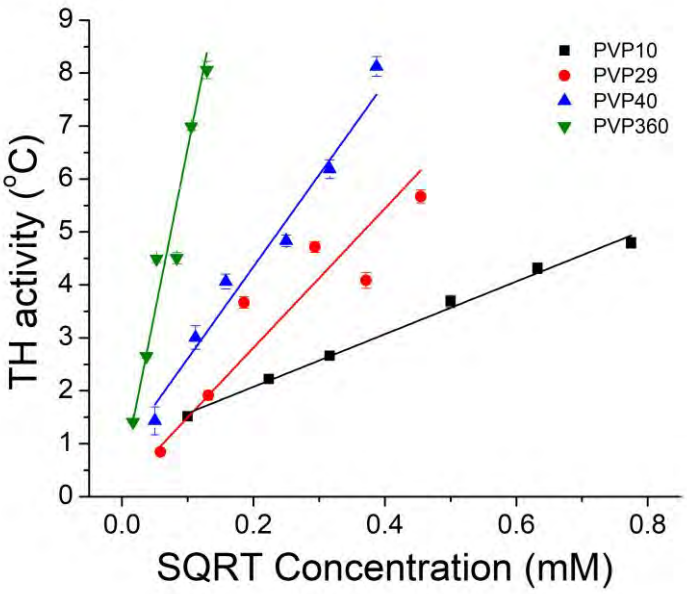


Figure 12: Graph of the thermal hysteresis activity as a function of the square root of the concnetration, for PVP at concentrations of 10, 29, 40, and 360 kDa

4.2: TH activity of zirconium acetate hydroxide on THF hydrates

ZRAH was added to a solution of water and THF at concentrations of 2, 5, 10, 15, and 20 mg/mL. At each concentration, a minimum of five crystals were isolated and their TH measured. As with PVP, I hypothesized that as the concentration of ZRAH increased, so would the inhibition activity.

This hypothesis again proved to be true, as seen in Figure 13. As with the PVP graph, the THF is compared to the square root of the molarity in order to achieve linearity. While ZRAH is a less effective inhibitor, as seen by the lower TH values despite being higher concentrations, it follows the same linear trend. With increasing concentration, the ZRAH becomes more effective.

While I attempted to measure concentrations of 30 and 40 mg/mL, the high levels of inhibitor caused the crystals to grow as sharp, thin rods (Figure 14). Due to the shape of these crystals, they were not able to be measured and, therefore, were not included in the graph.

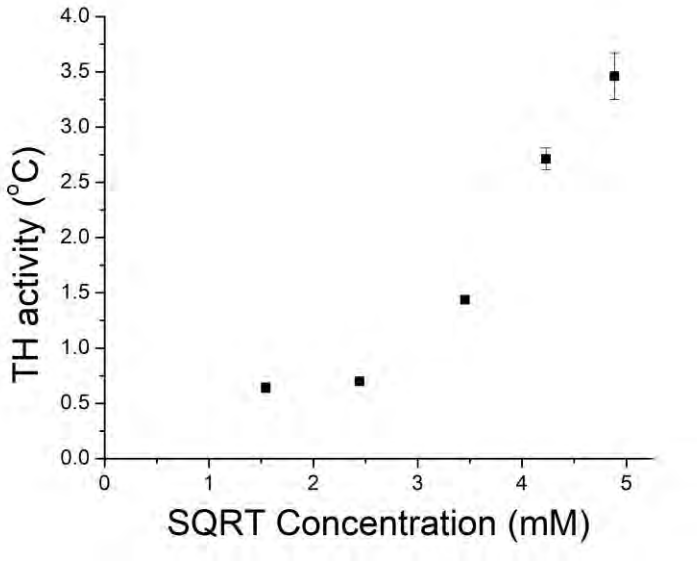


Figure 13: Graph of the thermal hysteresis activity as a function of the square root of the concentration for ZRAH

Additionally, I tried to measure the activity of ZRAH at different pH values. According to a study done by Mizrahy *et al.*, ZRAH has a larger thermal hysteresis when inhibiting ice at a more basic pH. In Mizrahy's study, ZRAH was tested at its baseline pH of 4.2 as well as a more acidic pH of 3.3 and a more basic pH of 4.7. To adjust the pH, the authors added 100 mM acetic acid or 100 mM sodium acetate. At higher pH values, the crystals exhibited a larger thermal hysteresis, while the more acidic ZRAH showed nearly no TH activity[11]. This could occur due to ZRAH self-oligomerizing at higher pHs[16]. While ZRAH over-

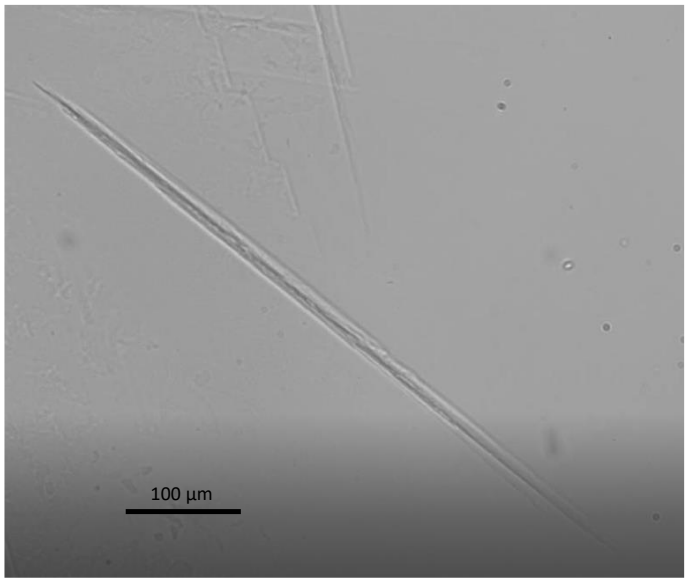


Figure 14: Picture of ZRAH crystal growth at 40 mg/mL

polymerizes at pHs above 4.7, and forms into thick gels, before this threshold, it simply forms longer ZRAH chains. This oligomerization may be necessary for binding to ice surfaces. Additionally, it can explain why Mizrahy et. al. observed a larger pH. Similar to PVP, where the larger polymers have higher TH values, ZRAH could be more effective in larger molecules[11].

Based on these findings with ice, I attempted the same technique to determine how pH affects the hydrates' inhibition efficacy of ZRAH. However, when adjusting the pH, a distinct white precipitate formed (Figure 15). This occurred regardless of the concentration of ZRAH, acetic acid, or sodium acetate and could not redissolve. Therefore, I was unable to obtain measurements at varied pHs of ZRAH.

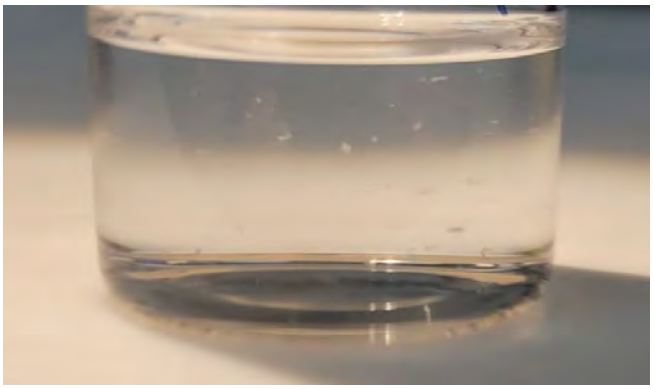

Figure 15: Picture of ZRAH solution precipitate

4.3: TH activity of antifreeze glycoproteins on THF hydrates

$AFGP_8$ and $AFGP_{1-5}$ were added respectively to a solution of water and THF. The TH with $AFGP_8$ was measured at concentrations 0.1, 0.5, 1, 3, and 5 mg/mL and the TH with $AFGP_{1-5}$ was measured at concentrations 0.05, 0.1, 0.5, 1, and 2 mg/mL. For each AFGP solution, at each concentration, a minimum of five crystals were isolated and their TH measured. Based on the published results of AFGPs with ice, I hypothesized that the TH of AFGP would increase with size. In this case, that means that $AFGP_{1-5}$ would have a higher TH activity than $AFGP_8$. This hypothesis was proven correct, as seen in Figure 16.

In addition to the concentration shown in the graph in Figure 16, I tested $AFGP_8$ and $AFGP_{1-5}$ at higher concentrations. Specifically, I tested $AFGP_8$ at 10 mg/mL and $AFGP_{1-5}$ at 14, 10, 5, and 3 mg/mL. However, at higher concentrations, the AFGPs either inhibit the formation of the hydrates entirely or cause the crystals to remain too small to obtain proper measurements.

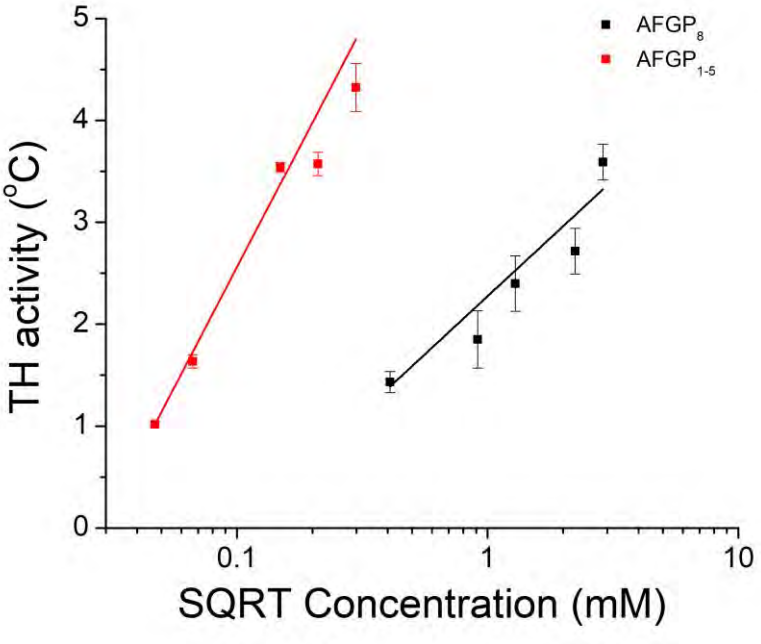


Figure 16: Graph of the thermal hysteresis activity as a function of the square root of the concentration, for $AFGP_8$ and $AFGP_{1-5}$

As with the other crystals, I determined the freezing point as the point the crystal exhibits rapid growth. However, with $AFGP_8$, the bursts of the crystals were much slower, making the calculations of the bursting points more difficult.

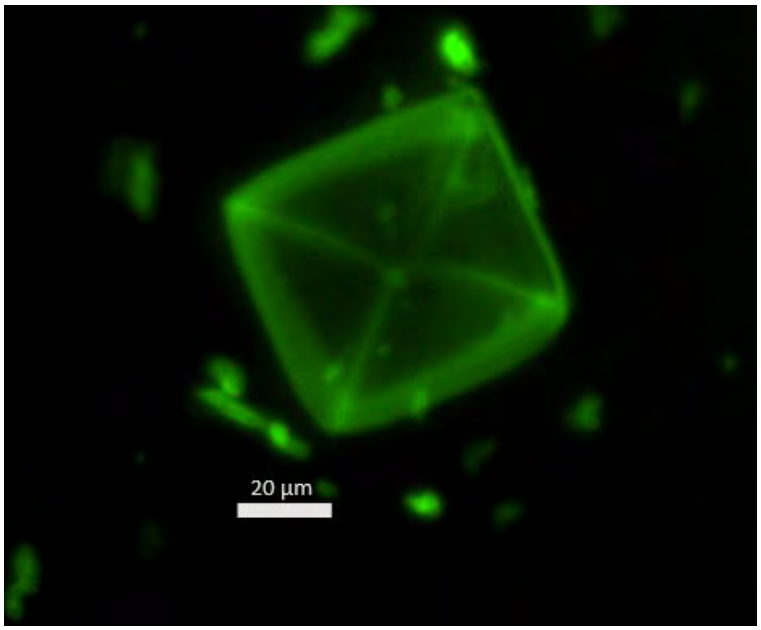


Figure 17: Picture of florescent labeled $AFGP_{1-5}$ proteins surrounding a THF hydrate

In addition to testing the inhibition, I wanted to test the mechanism of inhibition. In order to shed some light on AFGPs mechanism, my mentor added

fluorescently labeled AFGP$_{1-5}$ to THF hydrates. In Figure 17, you can see the fluorescently labeled proteins lining the surface of the crystal, illuminating the crystal structure.

4.4: TH activity of all inhibitors compared

To compare all the KHIs and AFGPs tested, I combined them all into one graph (Figure 18), which compares all the PVP, ZRAH, and AFGP values. As with all of the other graphs, this graph compares the TH activity to the square root of the molarity. Due to the large range in concentrations, the x-axis is on a logarithmic scale. By presenting all the data measured in one graph, one can appreciate the large range of inhibition efficacy (factor of 100 between the concentrations of ZRAH and PVP360), which is dictated mainly by the molecular weight of the KHIs.

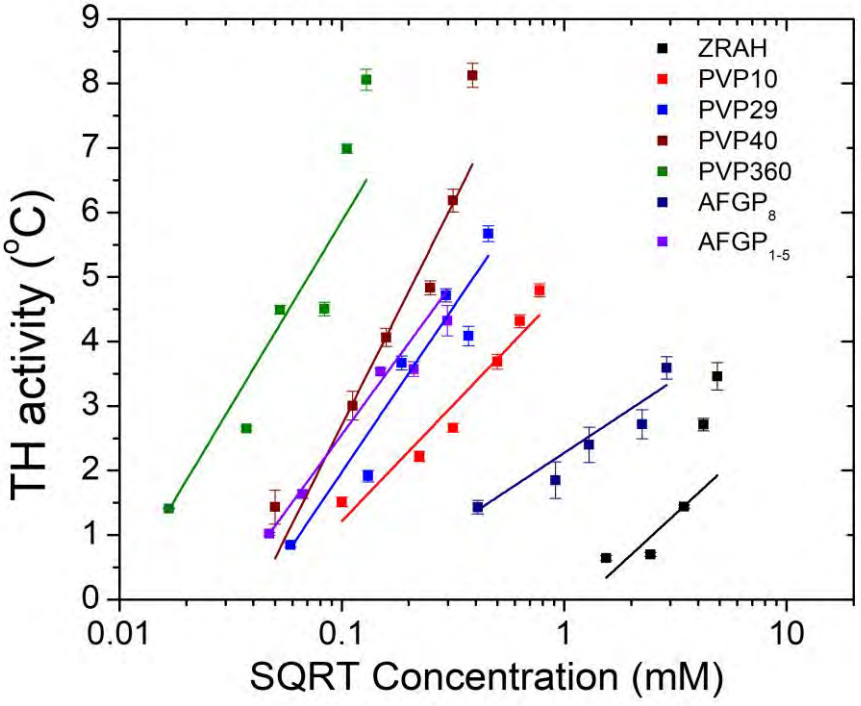


Figure 18: Graph of the thermal hysteresis activity as a function of the square root of concentration for PVP, ZRAH, and AFGPs

## 5. Discussion

### 5.1: Discussion of inhibitor results

When examining the inhibition effect of PVP, there is a clear correlation between the molecular weight and TH activity, as with increased polymer size, the inhibition increases. This correlation is likely due to the proposed mechanism of inhibition of KHIs that includes binding of the compound to the hydrates surface. The larger polymers cover a greater surface area and are therefore more effective at inhibition. However, the efficacy of PVP seems to plateau at a higher polymer length. PVP360, has a higher TH activity than PVP40, but the gap is not proportionate to the increased size of PVP360. PVP360 is 9 times as larger compared to PVP40, with 320 more monomer units, however the activity is only slightly higher. This could indicate that after a certain length, additional monomer units do not affect the efficacy of the inhibitor.

ZRAH, which has never been proven to inhibit THF hydrates, had clear inhibition capabilities. While the inhibition activity was low, ZRAH values were comparable to $AFGP_8$, which inhibits ice growth much more effectively compared to ZRAH. The limited activity could be due to the low molecular weight of ZRAH, and the possibility that ZRAH assembles in solution and forms self-assembled structures before binding to the crystal surface.

The AFGPs appear to inhibit THF hydrates in a similar manner as they inhibit ice growth. For ice, $AFGP_{1-5}$ has stronger inhibition than the smaller $AFGP_8$ and the same pattern was observed here with THF hydrates. Specifically, I hypothesize that the proteins adsorb to the surface of the hydrates, as they adsorb to ice surfaces and this binding event inhibits further growth. This is also supported by the fluorescence surrounding the crystal structure which would indicate that the proteins are adhering to the crystal's surface (Fig. 17).

In summary, these results provide strong evidence that the inhibition of THF hydrates by synthetic and biological KHIs is dictated by the molecular weight of the KHIs. The larger $AFGP_{1-5}$ is a slightly better inhibitor than PVP at comparable molecular weights. This is an important insight, as AFGPs probably bind to ice and THF hydrates via their disaccharide moiety, while PVP's γ-lactam ring fills empty cages on the surface of the hydrate.

## 5.2: Challenges with studying THF hydrates

Working with THF hydrates presents its own set of challenges, that are not present when working with ice samples. The first difficulty is forming THF hydrates. The THF and water are added at a specific ration, 1:3.3 THF to water, in order to encourage hydrate formation. However, even with this exact ratio, hydrates do not always form. This could occur for multiple reasons. Firstly, THF is a volatile liquid. Because THF evaporates quickly, all experiments must be done rapidly and if a THF solution is left out for more than about 10-20 minutes open, or 24 hours sealed, the THF evaporates, and hydrate formation is unlikely. Additionally, hydrate nucleation required low temperatures. As mentioned earlier, this usually occurs around -30 to -40 °C, although the solution occasionally requires lower temperatures to freeze over. This often occurs if the sample size is small. However, these low temperatures can be difficult to maintain.

In addition to the challenge of freezing hydrate crystals, it can be difficult to isolate crystals. At high concentrations of inhibitor, crystal nucleation can be inhibited, preventing the formation of crystals. If nucleation does occur, the high concentration often causes increased inhibition, so the crystals are too small to be measurable. However, isolating specific crystals is vital to obtaining proper measurements. If there are other hydrate crystals near the one being measured, they can

burst before the crystal being studied. This can result in the crystal being analyzed being overrun by growth of another crystal, which prevents a proper freezing point from being calculated.

Once a crystal is isolated, measurements can still be difficult to obtain due to the position of the crystal. The edges of the sample are thermodynamically favored to be colder than the center. Therefore, crystal growth tends to be thicker around the edges of the sample and isolated in those areas. However, there are often bubbles around the rim of the sample and their presence can obstruct the crystal and make it difficult to measure. Additionally, the orientation of the crystal can be important for obtaining reliable melting point measurements. Measuring a crystals melting point is usually done by examining the edges of the crystal and determining when the crystal stops shrinking. However, for some crystals, due to their position in the solution and the plane being observed, the melting is seen by the crystal thinning, instead of shrinking. This makes it impossible to accurately determine the melting point, and therefore calculate the TH.

References


1. Sloan ED. *Reviews Gas Hydrates: Review of Physical/Chemical Properties*.; 1998. https://pubs.acs.org/sharingguidelines

2. Kvenvolden KA. Gas hydrates-geological perspective and global change. *Reviews of Geophysics*. 1993;31(2):173-187. doi:10.1029/93RG00268

3. Sloan ED. *Fundamental Principles and Applications of Natural Gas Hydrates*.; 2003. www.nature.com/nature

4. Hammerschmidt EG. *Formation of Gas Hydrates in Natural Gas Transmission Lines*. Vol 144.; 1907. https://pubs.acs.org/sharingguidelines

5. Walker VK, Zeng H, Ohno H, et al. Antifreeze proteins as gas hydrate inhibitors. *Canadian Journal of Chemistry*. 2015;93(8):839-849. doi:10.1139/cjc-2014-0538

6. United States Environmental Protection Agency. Deepwater Horizon – BP Gulf of Mexico Oil Spill.

7. Anderson BJ, Tester JW, Borghi GP, Trout BL. Properties of inhibitors of methane hydrate formation via molecular dynamics simulations. *J Am Chem Soc*. 2005;127(50):17852-17862. doi:10.1021/ja0554965

8. Zhang JS, Lo C, Couzis A, Somasundaran P, Wu J, Lee JW. Adsorption of kinetic inhibitors on clathrate hydrates. *Journal of Physical Chemistry C*. 2009;113(40):17418-17420. doi:10.1021/jp907796d

9. Davies PL. Ice-binding proteins: A remarkable diversity of structures for stopping and starting ice growth. *Trends in Biochemical Sciences*. 2014;39(11):548-555. doi:10.1016/j.tibs.2014.09.005

10. Harding MM, Anderberg PI, Haymet ADJ. “Antifreeze” glycoproteins from polar fish. *European Journal of Biochemistry*. 2003;270(7):1381-1392. doi:10.1046/j.1432-1033.2003.03488.x

11. Mizrahy O, Bar-Dolev M, Guy S, Braslavsky I. Inhibition of Ice Growth and Recrystallization by Zirconium Acetate and Zirconium Acetate Hydroxide. *PLoS ONE*. 2013;8(3). doi:10.1371/journal.pone.0059540

12. Vlasic TM, Servio PD, Rey AD. THF Hydrates as Model Systems for Natural Gas Hydrates: Comparing Their Mechanical and Vibrational Properties. *Industrial & Engineering Chemistry Research*. 2019;58(36):16588-16596. doi:10.1021/acs.iecr.9b02698

13. Bar Dolev M, Braslavsky I, Davies PL. Ice-Binding Proteins and Their Function. *Annual Review of Biochemistry*. 2016;85:515-542. doi:10.1146/annurev-biochem-060815-014546

14. Braslavsky I, Drori R. LabVIEW-operated Novel Nanoliter Osmometer for Ice Binding Protein Investigations. *Journal of Visualized Experiments*. 2013;(72). doi:10.3791/4189

15. Soussana TN, Weissman H, Rybtchinski B, Drori R. Adsorption-Inhibition of Clathrate Hydrates by Self-Assembled Nanostructures. *ChemPhysChem*. 2021;22(21):2182-2189. doi:10.1002/cphc.202100463

16. Jutson JA, Richardson RM, Jones SL, Norman C. Small Angle X-ray Scattering Studies of Polymeric Zirconium Species in Aqueous Solution. *MRS Proceedings*. 1990;180:123. doi:10.1557/PROC-180-123